Chapter VII:

ARSENIC REMOVAL USING IMMOBILIZED AND ENCAPSULATED BACTERIA

7.1 General

Bioremediation can be carried out employing free cell (suspended culture) or an immobilized cell (attached growth) system (Swain et al., 2020). Unlike free cells, immobilized cells offer more significant advantages by providing low hydraulic retention time and higher biomass concentration availability per unit carrier volume. However, in both systems, microorganisms are directly exposed to adverse environmental conditions, which results in their decreased metabolic activity (Jaiswal et al., 2023b). Providing a protective cover to the microorganisms (immobilized on biochar) can help solve this problem, and encapsulation inside beads is an effective way to achieve this. PVA and SA beads have been widely used to encapsulate bacteria for the treatment of pollutants. PVA is a biodegradable, biocompatible polymer (Aljar et al., 2021) and reacts strongly with SA. Due to excellent chemical resistance, it does not cause any environmental pollution when used as a coating material (Amiri et al., 2023). SA can be extracted from brown algae and is a biodegradable copolymer that is non-toxic to bacteria (Baigorria et al., 2020). PVA-SA beads provide the advantage of easy separation and enhanced mechanical strength (Wen et al., 2018).

PVA or SA, when used separately, results in weak hydrogels and are prone to swelling, but their cross-linking with Ca^{2+} enhances the stability of the structure significantly (Zhang et al., 2022). Various studies by previous researchers have found that immobilized cells perform better than free cells in removing heavy metal(loid)s and several other pollutants (Al-Hasawi et al., 2020; Liu et al., 2018). Arsenic removal using bacteria immobilized on biochar or biochar encapsulated in PVA-SA beads has been reported by various researchers (Irshad et al., 2023; Ji et al., 2022; Jiang et al., 2024; Rind et al., 2023; Santos et al., 2012). However, arsenic removal by bacteria immobilized on biochar and further encapsulated in PVA-SA beads is very limited and highly underexplored. This study focused on the encapsulation of pre-immobilized bacteria on PSB in PVA-SA beads. It aimed to evaluate (i) preparation and characterization of biochar, (ii) arsenic [As(III) and As(V)] removal by using beads and (iii) the effects of temperature, pH and initial arsenic concentration on the removal efficiency. Bead strength and reusability were evaluated to assess the effectiveness of beads for arsenic removal.

7.2 Characterization of biochar

Differences between the observed surface topographies of PSB and MPSB surfaces are very obvious in their SEM images related to before and after adsorption (refer to Appendix B). The well-developed pores in MPSB can be attributed to the modification with $KMnO_4$

and KOH. The modification led to a combination of small pores into larger ones and hence, an increase in pore volume and specific surface area (An et al., 2021). This increase in specific surface area is responsible for an increase in the adsorption of arsenic.

The BET analysis revealed that specific surface area and pore volume increased after modification with $KMnO_4$ and KOH. Table 7.1 represents the parameters of surface area for PSB and MPSB. MPSB had more surface area, pore volume and lesser pore size than PSB, suggesting that modification did improve the surface characteristics of the biochar. This improvement resulted increased adsorption capacity by providing more adsorption sites (An et al., 2021).

The XRD pattern for PSB and MPSB (refer to Appendix B) indicated its crystallographic and physical properties. The shift in peak and loss in intensity at $2\theta = 22.62$ degrees represents that the surface of the biochar has become more amorphous and has resulted in an increase in pore volume and surface area.

FTIR analysis showed the functional groups present on the surface of biochar involved in arsenic removal. In PSB, peak at 3390 cm^{-1} corresponded to the presence of –OH groups of phenols or alcohols. Peaks at 2961 cm^{-1} and 1376 cm^{-1} and in the range of 500 cm^{-1} to 900 cm^{-1}, although very small, could be due to the stretching vibrations of –CH (Shakya et al., 2022; Wang et al., 2020), stretching at 1561 cm^{-1} may indicate the presence of C=C (Shan et al., 2020). The peaks in the range 1000 to 1200 cm^{-1} and 600 to 900 cm^{-1}, although small, corresponding to the C-O-C group of cellulose (Wang et al., 2020) and –CH bending vibrations (Shakya et al., 2022), respectively. The modification with $KMnO_4$ and KOH successfully introduced the active oxygen-containing functional groups and as a result, the peaks are enhanced at 1561 cm^{-1}, 1376 cm^{-1} and 3390 cm^{-1}. The findings for the modification of biochar are consistent with the previous studies (An et al., 2019). The properties of PSB have been listed in Table D1 (refer to Appendix D).

Table 7.1: Parameters related to the surface area for PSB and MPSB

	BET surface area (m^2/g)	**Pore volume (cm^3/g)**	**Pore size (nm)**
PSB	0.904	0.0047	20.796
MPSB	3.83	0.00987	10.306

7.3 Thermogravimetric analysis

Thermogravimetric analysis (TGA) was used for the determination of pyrolysis behavior and lignocellulosic composition of PS (Hai et al., 2021). Figure 7.1 represents the thermogravimetric (TG) curve for PS feedstock. The loss in mass has been represented in three stages. In stage I, the mass loss (6% - 7%) took place between room temperature to

~100°C, which can be due to loss of moisture content and degradation of volatile matter. In stage II, maximum mass loss (56% - 58%) took place between ~100°C to ~430°C, which can be attributed to the decomposition of hemicellulose and cellulose. In stage III, the mass loss (about 40%) happened between ~430°C and ~700°C, due to the decomposition of lignocellulose and the complex organic compounds formed during stage II (Gajera and Panwar, 2019). The mass loss observed in stage III was lower as compared to stage II, owning to a slower rate of loss of lignin (Gajera and Panwar, 2019), but higher than that in stage I. After 700°C, there was negligible change in mass loss, indicating a complete conversion of PS biomass to biochar.

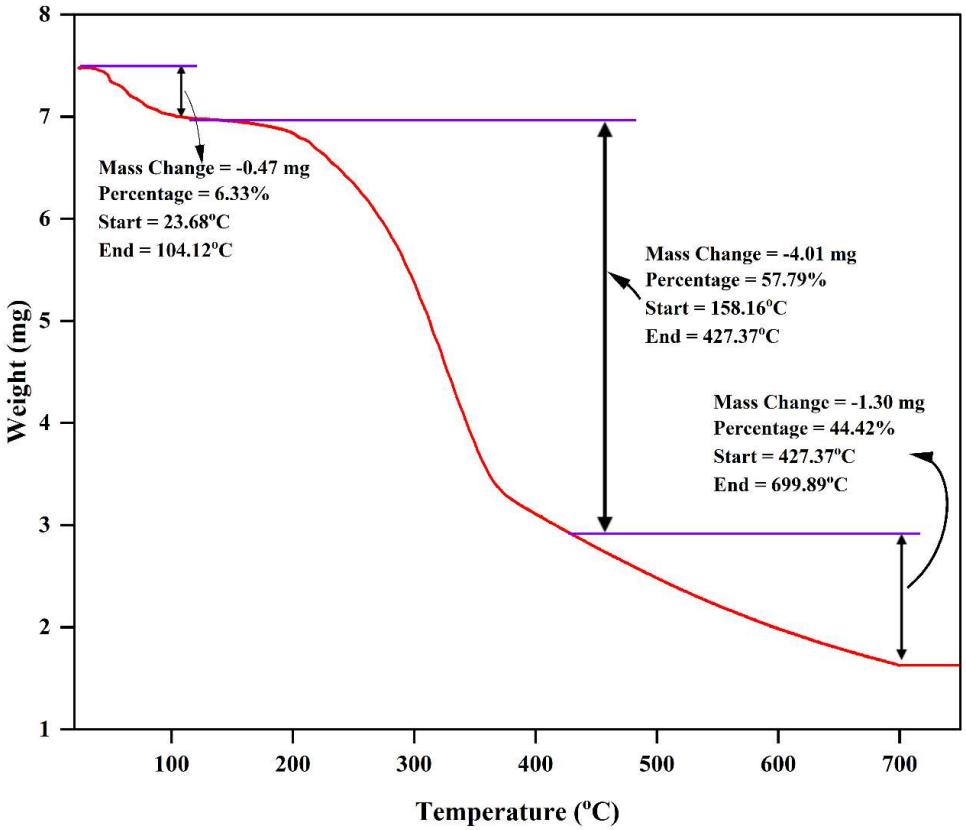

Figure 7.1: Thermogravimetric curve for PS feedstock

7.4 Effect of operating parameters on removal efficiency of biochar

As(III) and As(V) removal was dependent on the pH of solution as sorption increased with an increase in pH up to a certain limit and then decreased (Figure 7.2). The sorption of As(III) (75%) and As(V) (77.5%) peaked at pH 5 and pH 6, respectively for PSB, whereas for MPSB, the removal was highest at pH 6 for As(III) (86%) and As(V) (91.26%). MPSB was more effective in As(III) (increase of 11%) and As(V) (increase of 13.7%) removal as compared to PSB. As(III) exists in anionic form ($H_2AsO_3^-$) at higher pH (>9) (Mohan et al.,

2019) which results in repulsion between As(III) and surface functional groups (Giri et al., 2011). The increase in As(III) sorption efficiency in the acidic range and then further decrease could be attributed to deprotonation of hydroxyl groups. The results obtained here are similar to as observed by Wang et al. (2021) for rice straw biochar.

As(V) exists in the anionic form (as $H_2AsO_4^-$ and $HAsO_4^{2-}$) in the pH range 3 – 10 (Mukherjee et al., 2021). Positive charge develops at the sorbent surface at low pH due to protonation which further facilitates the removal of As(V) from the solution. The results of this study are in accordance with previously reported studies on PSB and other adsorbents used for arsenic removal (Mukherjee et al., 2021; Sattar et al., 2019). The sorption pattern followed by MPSB for As(III) and As(V) removal was also the same as that followed by PSB.

An adsorbent dose of 0.5 g/L was found to be most effective for both PSB and MPSB. However, sorption of As(III) and As(V) decreased after reaching a peak at 0.5 g/L [83.56% for As(V) and 81% for As(III)] for PSB but for MPSB there was a slight decrease in sorption after reaching the equilibrium at 0.5 g/L [90.68% for As(V) and 86% for As(III)]. The removal efficiency decreased for both PSB and MPSB as the initial concentration was increased from 0.1 mg/L to 1 mg/L. The removal efficiency reduced from 95.8% [MPSB - As(V)], 94% [MPSB – As(III)], 91.8% [PSB – As(V)], 88% [PSB – As(III)] at initial concentration of 0.1 mg/L to 87.32% [MPSB - As(V)], 78% [MPSB – As(III)], 68.52% [PSB – As(V)], 66% [PSB – As(III)] at initial concentration of 1 mg/L. When the initial concentration was further increased to 5 mg/L, the removal efficiency reduced to 40.23% [As(V)], 34% [As(III] for PSB and 57.35% [As(V)] and 43% [As(III)] for MPSB (not shown in graph). The increase in efficiency can be attributed to the availability of an adsorption site with an increase in adsorbent dose.

Negligible change in efficiency can be attributed to increased number of adsorption sites and lack of ion concentration resulting in agglomeration and cluster formation (Garg et al., 2019; Kumar and Bhattacharya, 2022; Shan et al., 2020). Removal efficiency increased with an increase in contact time till the equilibrium was reached. For PSB, sorption of As(III) and As(V) reached an equilibrium at 180 min and 60 min, respectively, whereas for MPSB it was 240 min for both As(III) and As(V), which may be due to repulsion between solute molecules at the adsorbent surface (Do and Lee, 2013; Mukherjee et al., 2021). Removal efficiency increased with an increase in temperature up to a certain extent [40^{o}C for As(III) – MPSB; 45^{o}C for As(III) – PSB, As(V) – PSB, As(V) – MPSB] and then, it decreased owning to immobilization of arsenic at lower temperatures. At higher

temperatures, arsenic detached from adsorbent site due to damaged binding sites and weakened binding forces (Alam et al., 2018; Kumar and Bhattacharya, 2022).

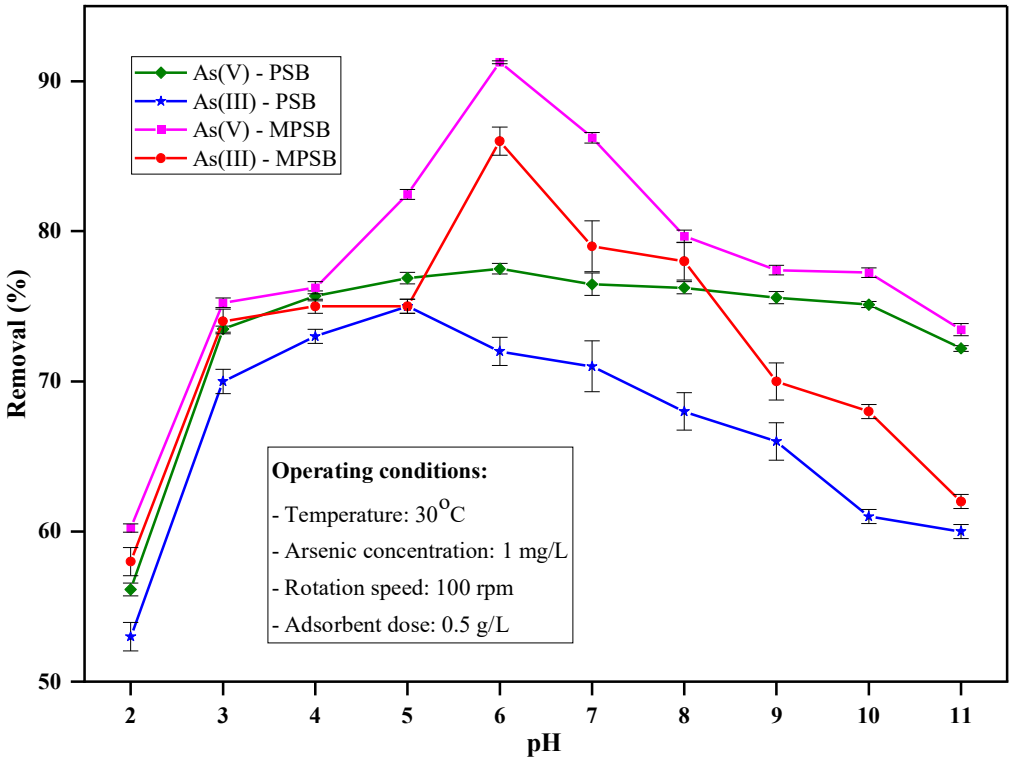

Figure 7.2: Influence of pH on the sorption of As(III) and As(V) on PSB and MPSB

Shaking speed was also found to affect the adsorption efficiency of arsenic on the biochar. The sorption efficiency increased with an increase in shaking speed up to 100 rpm and then it decreased for both PSB and MPSB. Increased stirring rate reduced the interaction between adsorption sites and ions thus, reducing the sorption efficiency (Alam et al., 2018).

7.5 Adsorption isotherm

Adsorption equilibrium was evaluated using Langmuir (refer to Appendix D) and Freundlich (refer to Appendix D) isotherm models and the parameters for the same have been shown in Table 7.2. The adsorption capacities obtained experimentally were 1.83 mg/g [for As(V)] and 1.76 mg/g [for As(III)] in case of PSB; while these values observed were 1.92 mg/g [for As(V)] and 1.88 mg/g [for As(III)] in case of MPSB. At higher concentrations (5 mg/L), the adsorption capacity increased to 4.02 mg/g [As(V)] and 3.40 mg/g [As(III)] for PSB and 5.74 mg/g [As(V)] and 4.30 mg/g [As(III)] for MPSB.

In Freundlich isotherm, the value of n for both the species, As(III) and As(V), was <1, which suggested that adsorption was favorable on both, PSB and MPSB. R_L value for

Langmuir isotherm was also found to be <1 for adsorption on both PSB and MPSB, suggesting that adsorption was favorable to Langmuir isotherm. However, correlation coefficients (R^2) for Freundlich isotherm was relatively higher [As(III) – PSB (0.9962); As(V) – PSB (0.9759); As(III) – MPSB (0.9697); As(V) – MPSB (0.9970)] as compared to Langmuir isotherm [As(III) – PSB (0.9712); As(V) – PSB (0.9058); As(III) – MPSB (0.9676); As(V) – MPSB (0.9499)] suggesting that Freundlich isotherm was a better fit for both, PSB and MPSB for arsenic adsorption, hence, the adsorption of arsenic was non-ideal and heterogeneous. Similar results have been reported for cadmium (Cheng et al., 2016), Acid Yellow 36 (Garg et al., 2019) adsorption on PSB. Sattar et al. (2019) have reported Langmuir isotherm to be a better fit as compared to Freundlich isotherm for arsenic adsorption on PSB.

Table 7.2: Isotherm parameters for sorption of As(III) and As(V) on PSB and MPSB

Model	**Parameters**				
		Q_m (mg/g)	**K_L**	**R^2**	**R_L [=1/(1+$K_L C_o$]**
Langmuir isotherm	As(III) – PSB	1.302	12.50	0.9712	0.074
	As(V) – PSB	1.031	24.87	0.9058	0.038
	As(III) – MPSB	1.455	23.61	0.9676	0.041
	As(V) – MPSB	1.455	34.53	0.9499	0.028
Freundlich isotherm		**K_f ($mg^{1-1/n} \cdot L^{1/n}/g$)**	**n**	**R^2**	
	As(III) – PSB	2.102	0.5847	0.9962	
	As(V) – PSB	2.653	0.5251	0.9759	
	As(III) – MPSB	2.637	0.6896	0.9697	
	As(V) – MPSB	3.675	0.5754	0.9970	

7.6 Kinetic modeling

The sorption kinetic data was fitted to pseudo-first order, pseudo-second order, Elovich and intra-particle diffusion model (refer to Appendix D). Table 7.3 shows the kinetic parameters of different models. The R^2 value of sorption for As(III) and As(V) was very close to 1 for pseudo-second order kinetics suggesting that chemisorption could be the rate-determining

step and the amount of sorption sites available affects the adsorption efficiency of PSB and MPSB (Garg et al., 2019; Sattar et al., 2019; Shi et al., 2023).

Elovich model proposes chemisorption with negligible desorption and is suitable for heterogeneous surfaces. In the present study, R^2 values of the model for both PSB and MPSB suggested chemisorption. The value of initial adsorption rate (α) showed an erratic behavior as the value obtained was very high and this could indicate that the initial rate of adsorption of arsenic on biochar was very high. Similarly, high values of α have been reported by López-Luna et al. (2019). β is also related to surface coverage and chemisorption activation energy, implying a heterogeneous distribution of sites with varying activation energies with surface coverage. Since the curve for Elovich model does not pass through the origin, a boundary layer control can be assumed to be related to the rate-controlling mechanism (Rahman et al., 2019).

Intra-particle diffusion involves two phenomena, mass transfer through film diffusion and consequent intra-particle diffusion and it is assumed that both processes take place simultaneously when the straight line does not pass through the origin (Sawood and Gupta, 2020). This model will be limiting step only when C = 0, but in this study, C > 0, which suggests that adsorption occurs within a short period of time for both PSB and MPSB (Sharma et al., 2018), which was also the case in Elovich model. The R^2 values for MPSB were closer to 1 compared to that of PSB in all cases except for pseudo-first order, which indicates better adsorption of arsenic in the case of MPSB as compared to PSB. The linear nature of the model indicated the involvement of intra-particle diffusion in the sorption mechanism. However, since the plot does not pass through the origin, it can be inferred that intra-particle diffusion was not the sole rate-limiting step. Since, the value of R^2 for pseudo-second order and intra-particle diffusion was very close, it can be concluded that any one model cannot describe the sorption mechanism alone. However, based on R^2 values, pseudo-second order was found to be a better fit for the sorption process.

7.7 Thermodynamic study

The thermodynamic study was used to confirm the spontaneity of the adsorption process. Several thermodynamic parameters such as ΔH (standard enthalpy change), ΔS (standard entropy change) and ΔG (standard Gibbs free energy) have been calculated using equation 7.1 (Banerjee et al., 2008):

$$\Delta G = -RT \ln K \qquad \text{---- (7.1)}$$

where, R = gas constant; T = temperature (Kelvin); K = equilibrium thermodynamic constant.

Table 7.3: Kinetic parameters for sorption of As(III) and As(V) on PSB and MPSB

Model	Parameters				
		Q_e (mg/g) (Experimental)	Q_e (mg/g) (Calculated)	R^2	K_1 (h^{-1})
Pseudo-first order	As(III) – PSB	1.240±0.0372	0.757	0.9274	0.0208
	As(V) – PSB	1.433±0.0214	1.416	0.9766	0.0882
	As(III) – MPSB	1.340±0.0174	0.1597	0.7946	0.0077
	As(V) – MPSB	1.474±0.0442	0.757	0.7110	0.0071
		Q_e (mg/g) (Calculated)	K_2 (g/mg-h)	R^2	
Pseudo-second order	As(III) – PSB	1.522±0.009	0.053	0.9985	
	As(V) – PSB	1.498±0.011	0.131	0.9981	
	As(III) – MPSB	1.721±0.024	0.033	0.9863	
	As(V) – MPSB	1.798±0.021	0.043	0.9884	
		α (mg/g-h)	β (g/mg)	R^2	
Elovich model	As(III) – PSB	1.37E+18	78.74	0.9010	
	As(V) – PSB	1.02E+28	69.44	0.8384	
	As(III) – MPSB	7.62E+18	76.92	0.9569	
	As(V) – MPSB	2.39E+25	78.74	0.9368	
		K_p (mg/g-$h^{1/2}$)	C (mg/g)	R^2	
Intra particle diffusion	As(III) – PSB	0.1326±0.0121	0.2860±0.0671	0.9600	
	As(V) – PSB	0.1522±0.0197	0.3732±0.1096	0.9221	
	As(III) – MPSB	0.1321±0.0091	0.3312±0.0508	0.9765	
	As(V) – MPSB	0.1309±0.0074	0.5043±0.0412	0.9841	

The values of ΔH and ΔS were calculated from the slope and intercept from a plot between 1/T and lnK (refer to Appendix D). The parameters for thermodynamic assessment have been represented in Table 7.4. The negative values of ΔG at different temperatures confirmed that the adsorption process was spontaneous for both PSB and MPSB and a decrease in the value of ΔG with an increase in temperature confirms the increase in spontaneity with an increase in temperature. The value of ΔG for As(V) was lower for both PSB and MPSB than that of As(III), which indicated that the adsorption of As(V) was easier as compared to As(III). The positive values of ΔH and ΔS confirm the endothermic nature of the process. A positive value of ΔS indicates the increase in randomness of the biochar-metalloid interface owing to the random distribution of arsenic on the biochar. Typically, the value of ΔH lies between 20.9–418.4 kJ/mol for the heat of chemical reactions (Sawood and Gupta, 2020), and in this study also, the value of ΔH was in this range, which indicates that the adsorption of arsenic on PSB and MPSB was through chemisorption. Based on the thermodynamic data (ΔG values), it was observed that the process was feasible at all temperatures.

Table 7.4: Thermodynamic parameters for adsorption of arsenic on PSB and MPSB

Thermodynamic parameters	Temperature (K)	As(III) - PSB	As(V) - PSB	As(III) - MPSB	As(V) - MPSB
Standard Gibbs free energy (ΔG kJ/mol)	298	- 3.69	- 3.91	- 4.05	- 4.68
	303	- 4.93	- 5.18	- 4.93	- 5.50
	308	- 5.32	- 5.37	- 5.48	- 6.31
	303	- 5.41	- 5.61	- 5.93	- 7.15
	318	- 5.84	- 5.92	- 5.17	- 7.77
Standard enthalpy change (ΔH kJ/mol)		24.67±7.24	22.63±7.25	15.49±10.61	41.96±1.96
Standard entropy change (ΔS J/mol)		96.47±2.83	90.37±2.83	66.94±4.14	156.54±6.37

7.8 Adsorption mechanism of arsenic on biochar

Arsenic adsorption on PSB can occur through several mechanisms, including physical adsorption, chemical adsorption, and electrostatic attraction. The possible mechanism of arsenic adsorption on the biochar surface may include all three mechanisms. The results showed that the adsorption capacity of MPSB was better than that of PSB, owing to its higher surface area after modification. Isotherm and kinetic study revealed that the arsenic adsorption on biochar was possibly multilayer and of a chemical nature. FTIR analysis revealed the presence of several functional groups on the surface of the biochar, including –OH, -CH, -COOH and C=C. These groups can bind with arsenic and help in the adsorption process. The –OH group can either form hydrogen bond leading to physical adsorption, or can act as a Lewis base and donate electron pairs to the arsenic species, resulting in the formation of a chemical bond between arsenic and biochar.

Furthermore, the presence of –OH groups can increase the negative charge density on the biochar surface, which in turn can enhance the attraction of the positively charged arsenic species to the biochar surface (Wang et al., 2021). –CH can contribute to the adsorption of arsenic through hydrophobic interactions. Also, the presence of -CH groups can decrease the overall surface charge of the biochar, which can affect the electrostatic attraction between the biochar surface and arsenic. C=C can act as a site for electron donation resulting in the formation of a chemical bond between the arsenic species and the biochar surface. The presence of the double bond also introduces a degree of unsaturation to the biochar surface, which can increase the reactivity of the biochar towards arsenic. In addition, K^+ group introduced through modification plays a role in ion exchange and can also help in arsenic removal through co-precipitation (Shan et al., 2020). A conceptual diagram of different mechanisms of arsenic adsorption on biochar has been shown in Figure 7.3.

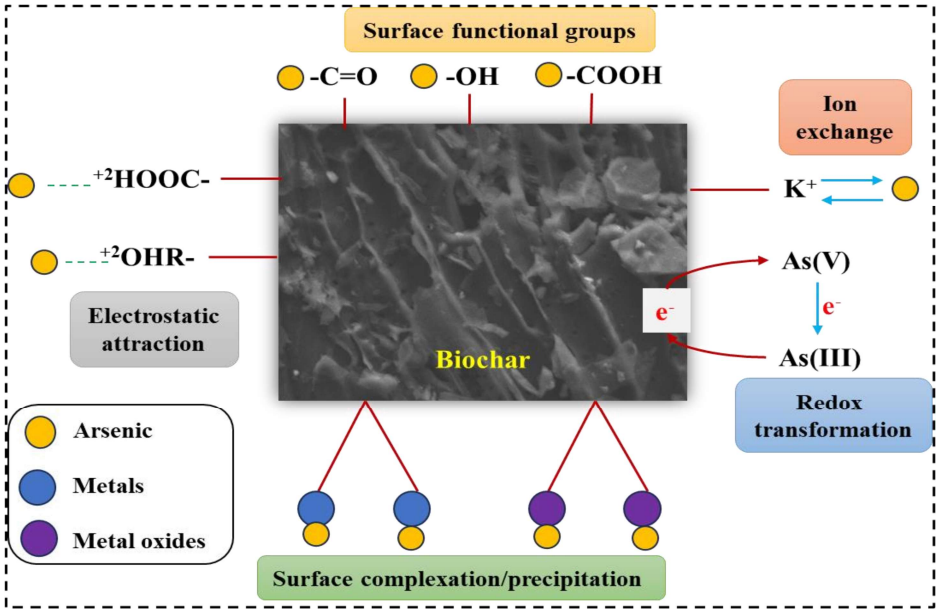

Figure 7.3: Conceptual diagram of arsenic adsorption mechanisms on biochar

7.9 Regeneration of biochar

Regeneration of biochar is very essential to explore its reusability and make it more cost-effective. In the present work, 0.1 M NaOH solution was used for the desorption study. It was observed that removal efficiency decreased significantly after three cycles. After regeneration, removal efficiency reduced to ~60% and ~70% for PSB and MPSB respectively, after three cycles. Excess of alkali introduces –OH in the solution, which is assumed to replace As(III)/As(V) through a ligand exchange reaction (Priyadarshni et al., 2020). After regeneration, the removal efficiency for As(V) and As(III) reduced from 82% to 61% and 79% to 55% for PSB, from 91% to 72% and 87% to 64% for MPSB. A detailed regeneration study using other regenerating solutions, such as H_2SO_4, HCl, HNO_3, ethylenediaminetetraacetic acid (EDTA), etc., should also be explored further.

Acids destroy the mineral structure of biochar after every cycle owing to their reaction with the mineral structure (Alsawy et al., 2022) and, in most cases, outperform alkalis. However, in general, HNO_3 is found to be a better desorbing agent as compared to HCl, as HCl forms precipitates leading to re-adsorption. Also, the acidic erosion may result in an increase in the surface area of the adsorbent, thus resulting in an enhanced adsorption cycle, making the process more cost-effective and environment-friendly (Alsawy et al., 2022).

7.10 Disposal of spent biochar

The use of biochar as an adsorbent is an environment-friendly method of arsenic treatment. However, the spent biochar (after three cycles of regeneration) loaded with arsenic should be given due consideration before its disposal. The arsenic-loaded biochar can be used for metal recovery, and the process may also be commercialized at a large scale (economic analysis for the recovery needs to be investigated in detail). The metal-devoid biochar can then be considered for disposal in agricultural fields as soil amendments to increase soil fertility, for carbon sequestration, to capture greenhouse gases, etc. (Xiang et al., 2021). The modified biochar was found to be effective in the removal of arsenic, and it can also be extended to other pollutants, thus making it more environment-friendly. PS, being a plant biomass, has low polyaromatic hydrocarbon precursors, and since the biochar was prepared through slow pyrolysis, the harmful contents are low and, hence, pose lower eco-toxicity. However, the negatives of the modification, such as the long-term effect of the biochar, should not be overlooked and need to be investigated further.

7.11 Effect of PVA, SA and $CaCl_2$ content on bead formation and arsenic removal efficiency

Determination of optimal chemical composition is one of the most important steps in manufacturing stable and strong beads to obtain maximum removal efficiency. The arsenic removal efficiency was found to vary when PVA, SA, or $CaCl_2$ concentrations were varied. PVA content varied between 1 – 9% and it was observed that arsenic removal increased with an increase in PVA% (up to 5%) and then decreased with a further increase in PVA content. Arsenic removal was 60.68 ± 0.48% at 1% PVA, 91.89 ± 0.69% at 5% PVA and 85.20 ± 0.21% at 9% PVA (refer to Appendix D). When SA content was varied from 0.5 – 2.5%, arsenic removal varied from 80.35 ± 0.62% (at 0.5% SA) to 95.54 ± 1.11% (at 2.0% SA) and 87.88 ± 0.68% (at 2.5% SA) (refer to Appendix D). With variation in $CaCl_2$ content between 0.5 – 2.0%, arsenic removal increased with an increase in $CaCl_2$ content up to 1.0% and then decreased. Removal efficiency increased from 87.88 ± 0.68% at 0.5% $CaCl_2$ to 95.83 ± 0.63% at 1.0% $CaCl_2$ and then decreased to 72.99 ± 0.80% at 2.0% $CaCl_2$ (refer to Appendix D).

PVA hydrogels are highly porous and vastly employed as bacteria carriers. Alginate has a good affinity towards calcium ions and the matrix can be used as an inoculant carrier (Farid et al., 2023). PVA concentration affects the strength, stability of beads and mass transfer efficiency of nutrients and may have the maximum effect (compared with SA and Ca^{2+}) on arsenic removal. Higher PVA content also increases the number of cross-linking

sites which subsequently enhances the expansion rate of gel as well as retention of biomass on the gel (Wang et al., 2021). An increase and decrease in arsenic removal efficiency with a change in PVA concentration can result from increased pore size at lower PVA% and decreased pore size, increased viscosity and increased resistance to mass transfer at higher PVA% (Ruan et al., 2018; Xu et al., 2019). However, several researchers have reported even higher PVA concentrations as the optimum content (Bialik-Wąs et al., 2021; Niu et al., 2021; Szczęsna-Antczak and Galas, 2001; Zain et al., 2011; Zhao et al., 2022).

SA prevents the agglomeration of beads and improves their surface properties. In this case, beads could not maintain their stability and ruptured easily at lower SA content, and at higher SA concentration, the removal efficiency decreased due to hindrance in substrate diffusion through the beads (Ruan et al., 2018). However, SA content, as low as 0.3% and 0.8%, have also been reported in previous studies (Ruan et al., 2018; Xu et al., 2019). Ca^{2+} serves as the crosslinking agent. In presence of Ca^{2+}, SA undergoes further crosslinking and inhibits water absorption (Bialik-Wąs et al., 2021). Ca^{2+} interacts ionically with alginate units, resulting in a 3D structure called "egg box" (Bajpai and Sharma, 2004). The interaction involved in crosslinking has been shown in Figure 7.4.

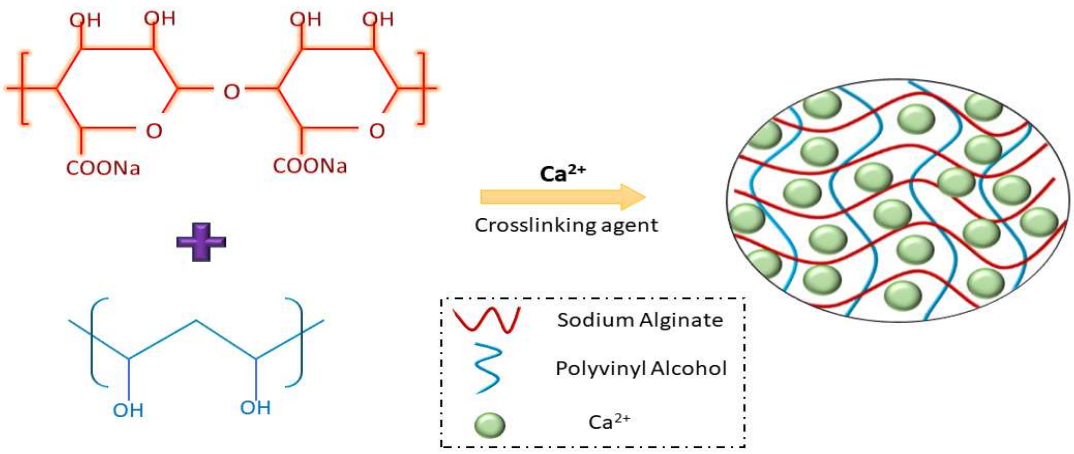

Figure 7.4: Schematic diagram of crosslinking of PVA and SA with Ca^{2+} for formation of beads [adopted and modified from Zhou et al. (2018)]

7.12 Effect of temperature and pH on efficiency of arsenic removal

The effect of temperature and pH on arsenic removal efficiency has been shown in Figure 7.5 (A) and Figure 7.5 (B) respectively. Temperature plays a crucial role in the performance of the bacteria. It is one of the important parameters that control microbial activity, diffusion rate, metabolic rate and solubility (Singh et al., 2022). Hence, the performance of bacterial

strains was evaluated at different temperatures (20 – 40ºC). The removal efficiency of As(III) and A(V) using IBT and IBK, respectively increased with an increase in temperature up to 30ºC and then decreased with a further increase in temperature. As(V) removal using IBK varied from 87.66 ± 0.62% (at 20ºC) to 77.22 ± 0.87% (at 45ºC) with maximum removal of 90.85 ± 0.65% (at 30ºC).

As(III) removal using IBT varied from 80.78 ± 0.57% (at 20ºC) to 77.46 ± 1.05% (at 45ºC) and the highest removal of 87.86 ± 0.66% (at 30ºC). When both bacteria were used in combination, that is, beads of IBK+IBT, removal efficiency for As(V) varied from 83.97 ± 0.34% (20ºC) to 78.22 ± 0.40% (45ºC) with peak removal of 92.55 ± 0.03% at 30ºC. For As(III), it varied from 84.61 ± 0.48% (20ºC) to 77.69 ± 0.58% (45ºC) with maximum of 92.30 ± 0.40% at 30ºC. A decrease in the removal efficiency by bacterial strains at higher temperatures can be attributed to decreased microbial activity at elevated temperatures. Also, an increase in temperature may result in the denaturation of protein, which results in enzymatic deactivation and it further leads to reduced metabolism of bacteria (Singh et al., 2022).

As(III) and As(V) removal using IBT and IBK were found to vary with pH also. As(III) removal varied from 78.55 ± 0.47% at pH 3 to 68.44 ± 0.34% at pH 11, whereas As(V) removal varied from 69.03 ± 0.45% at pH 3 to 75.55 ± 0.42% at pH 11. Maximum removal efficiency obtained was 89.75 ± 0.20% at pH 7 for As(III) with IBT and 93.52 ± 0.41% at pH 7 for As(V) using IBK. With beads of IBK+IBT, As(V) removal varied from 69.38 ± 0.32% (pH 3) to 82.00 ± 0.21% (pH 11) with maximum removal at pH 8 (96.48 ± 0.01%). As(III) removal efficiency varied from 68.31 ± 0.04% (pH 3) to 79.26 ± 0.49% (pH 11), with maximum removal at pH 8 (95.31 ± 0.22%). Most bacteria lose activity at extreme pH conditions due to protein denaturation (Bera et al., 2017).

PVA-SA beads at lower pH (3 and 4) are more porous with higher diffusion rates; however, low pH required for better crosslinking may adversely affect the functionality of the bacteria (Candry et al. 2022), which may account for reduced removal efficiency at lower pH. Immobilized *Bacillus* XZM on corn cobs biochar was found to be most effective at pH 6.9 by Irshad et al. (2023). Vu et al. (2017) reported that As(V) adsorption by magnetic graphene oxide encapsulated in alginate was not significantly affected by pH as Ca^{2+} controlled the local pH. Water treatment residues-alginate beads were found to have reduced efficiency for As(III) and As(V) removal at pH 7 by Ociński et al. (2016).

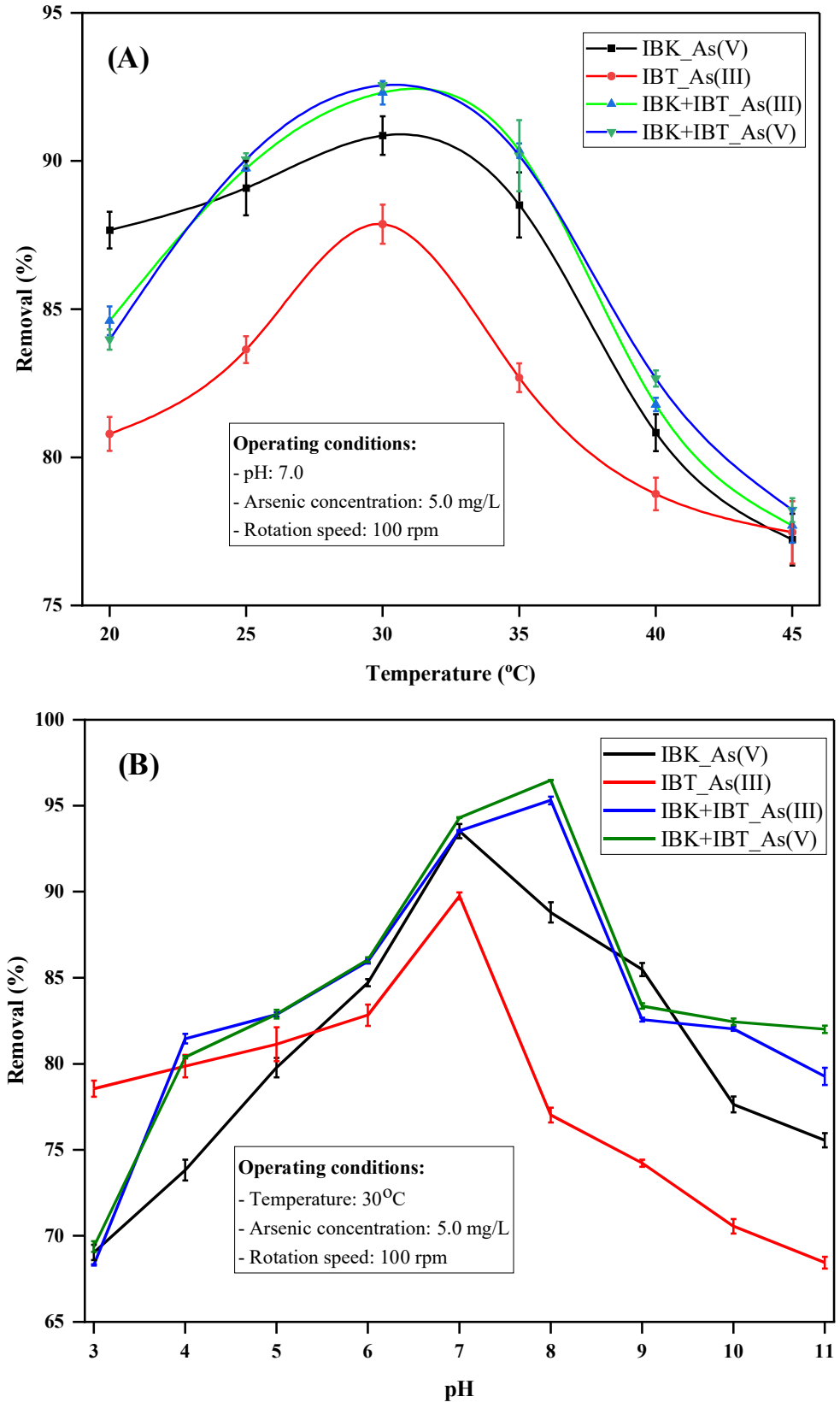

Figure 7.5: Effect of **(A)** Temperature and **(B)** pH on arsenic removal efficiency using IBK, IBT and IBK+IBT beads

7.13 Effect of initial arsenic concentration

With an increase in initial arsenic concentration (C_i), removal efficiency first increased and then decreased with a further increase in concentration (Figure 7.6). For IBK, removal efficiency varied from 88.23 ± 1.12% (C_i = 0.5 mg/L) to 34.37 ± 0.97% (C_i = 100 mg/L), whereas for IBT it ranged from 86.91 ± 0.31% (C_i = 0.5 mg/L) to 27.79 ± 0.87% (C_i = 100 mg/L). The maximum As(V) removal efficiency obtained was 92.29 ± 0.51% (C_i = 5 mg/L) using IBK and 91.71 ± 0.05% (C_i = 5 mg/L) for As(III) using IBT. With IBK+IBT beads, As(V) removal efficiency varied from 87.16 ± 0.09% (C_i = 0.5 mg/L) to 78.76 ± 0.09% (C_i = 100 mg/L) with maximum removal of 93.63 ± 0.09% (C_i = 10 mg/L). For As(III), the removal efficiency varied from 86.05 ± 0.06% (C_i = 0.5 mg/L) to 71.69 ± 0.19% (C_i = 100 mg/L) with maximum removal of 91.20 ± 0.05% (C_i = 5 mg/L). The decrease in removal efficiency could be due to suppressed bacterial activity at higher arsenic concentrations. However, the removal of arsenic was higher for beads in comparison to suspended bacteria or biochar.

The increased removal capacity can be attributed to the fact that PVA-SA beads provide greater surface area than biochar alone. Also, the functional groups present in PVA-SA are capable of forming chemical bonds that can help remove arsenic. The removal efficiency in case of mixed bacteria was significantly higher than the individual strain. This could be due to the increased bacterial concentration in beads, their adaptation to potentially toxic substances, or the synergistic effects of the mixed culture (Wen et al., 2021). Similar results have been observed for the removal of aromatic hydrocarbons, where mixed culture of bacteria was found to have higher removal efficiency than a single strain of bacteria (Kumari et al., 2018; Patowary et al., 2016; Wanapaisan et al., 2018; Zhong et al., 2011).

7.14 Comparison of removal efficiencies of various combinations

Figure 7.7 represents the comparative study for bioremediation of arsenic using PSB [PSB_As(III) and PSB_As(V)], free cell bacteria [As(III)_TY6 and As(V)_K7Pb], bacteria immobilized on biochar [IB_As(III)_TY6 and IB_As(V)_K7Pb] and beads of bacteria immobilized on biochar [IBK_As(V), IBT_As(III), IBK+IBT_As(V) and IBK+IBT_As(III)]. Free cell bacteria showed high removal efficiency for both As(III) and As(V) at lower concentrations of 50 µg/L and 100 µg/L. However, removal efficiency significantly decreased with an increase in concentration (Figure 7.7), and time for remediation also increased. A similar trend was observed for PSB, removal efficiency decreased from 91.80 ± 3.21% (C_i = 100 µg/L) to 11.26 ± 0.39% (C_i = 10 mg/L). The efficiency significantly increased in the case of IB_As(III)_TY6 and IB_As(V)_K7Pb

compared to free-cell or PSB. However, it decreased to 2.77 ± 1.01% [IB_As(III)_TY6] and 3.67 ± 0.47% [IB_As(V)_K7Pb] at higher concentrations (C_i = 100 mg/L). The encapsulated bacteria could remove arsenic (34.37 ± 0.97% with IBK and 27.79 ± 0.87% with IBT) even at higher concentrations of 100 mg/L.

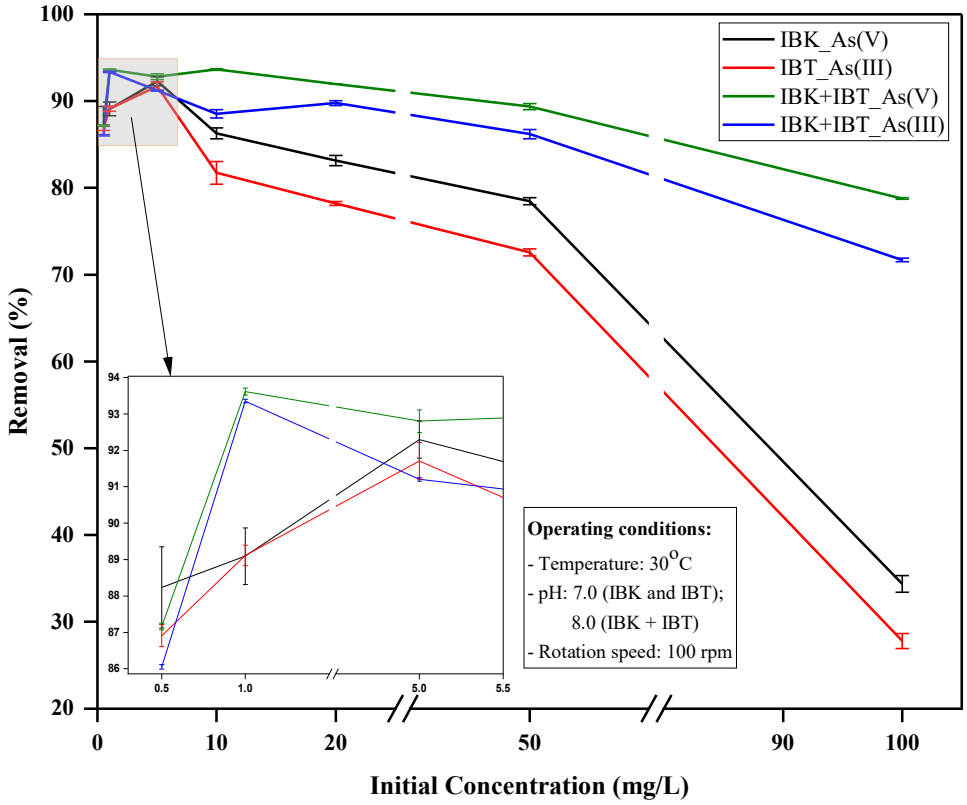

Figure 7.6: Effect of initial arsenic concentration on removal efficiency of IBK, IBT and IBK+IBT beads

The decline in the removal efficiency of free-cell bacteria employed that increased arsenic concentrations are toxic to the cell. For PSB, the decrease in removal efficiency could be due to reduced adsorption sites with increased arsenic concentration. Higher removal efficiency for encapsulated bacteria may result from its protection from direct exposure to toxic environments. Also, higher concentration increases the chances of collision between ions and gel, resulting in enhanced adsorption (Jiang et al., 2013). However, excessive concentration blocks the active sites, which may lead to decreased removal efficiency in the case of PSB (Li et al., 2021). SA-polyvinyl oxide-ceramic nanomaterial gels were found to have a removal rate of 67.42% for As(III) from wastewater (Li et al., 2021). Similar trends were also observed for other pollutants.

Zhang et al. (2020) and Xiang et al. (2023) found that bacteria immobilized on biochar and PVA/SA/Biochar beads had higher removal efficiencies than bacteria of

PVA/SA alone for cresol and thiamethoxam, respectively. Also, the higher efficiency of the beads may be attributed to the fact that in this case, bioaccumulation by bacteria, adsorption by biochar and adsorption by PVA-SA beads takes place as opposed to only bioaccumulation in free-cell bacteria or only adsorption in case of PSB.

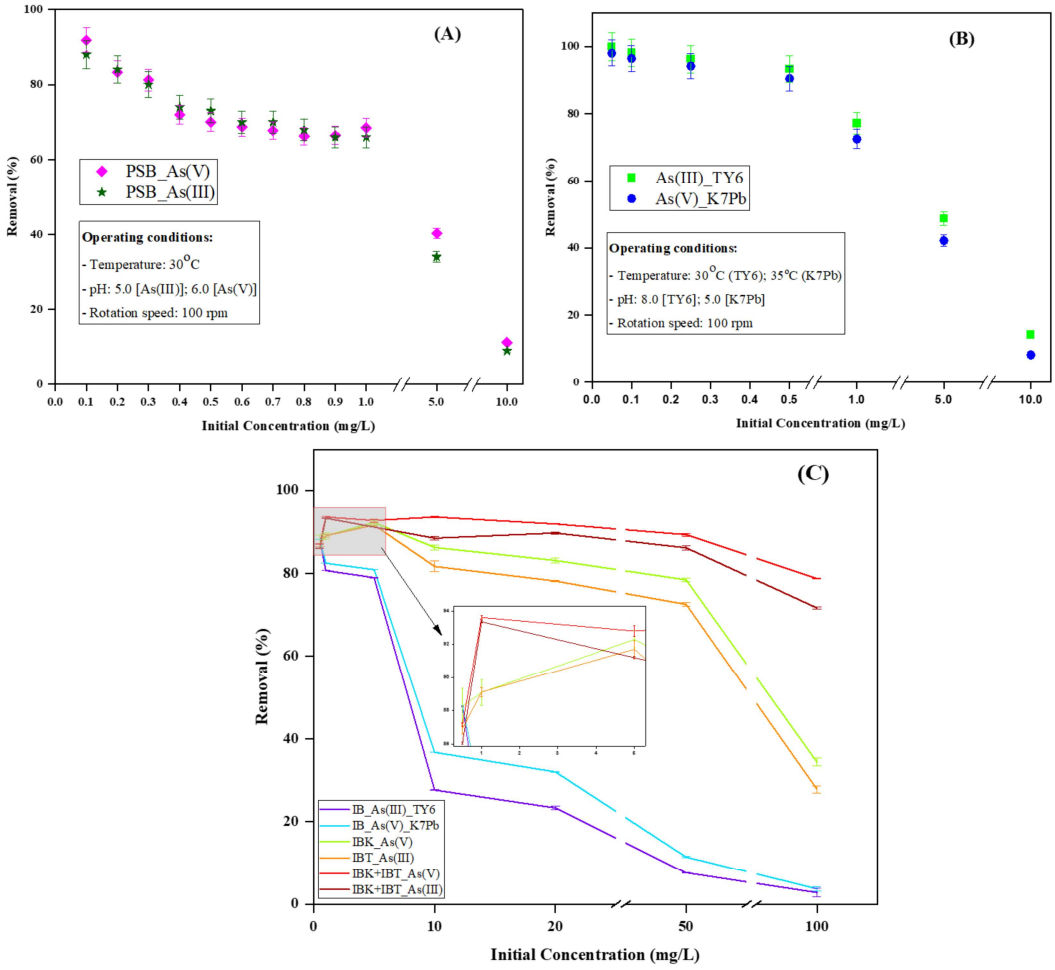

Figure 7.7: Comparative study for arsenic removal using **(A)** PSB [PSB_As(III) and PSB_As(V)]; **(B)** free-cell bacteria [As(III)_TY6 and As(V)_K7Pb]; **(C)** bacteria immobilized on biochar [IB_As(III)_TY6 and IB_As(V)_K7Pb] and beads of bacteria immobilized on biochar [IBK_As(V), IBT_As(III), IBK+IBT_As(V) and IBK+IBT_As(III)]

7.15 Characterization of beads

The outer surface of the bead was smooth, dense and non-porous. The internal structure was found to be rough and porous, and bacterial growth was observed on the surface of biochar, implying that the mechanical properties provided favorable conditions for the growth and proliferation of bacteria. Due to the formation of hydrogen bonds between

oxygen-containing groups in biochar and -OH groups in PVA, a strong interaction exists between PVA and biochar. This causes disruption of hydrogen bonds of PVA and a decrease in their attachment, resulting in increased porosity of the beads. This possibly lowered the diffusion resistance and increased the mobility of nutrients (Jaiswal et al., 2023b). The SEM images of the beads have been shown in Figure B3 (refer to Appendix B).

EDX analysis was used to confirm the presence of arsenic in the used samples (after treatment) (refer to Appendix B). The presence of arsenic after use employed that it was adsorbed on the beads. Both IBT and IBK showed the absence and presence of arsenic before and after their use. The C, Na and O peaks may possibly be associated with the -OH and -COONa groups linked with PVA and SA. The presence of Ca and Cl_2 was linked with the crosslinking agent, $CaCl_2$.

FTIR analysis showed the presence of functional groups on the surface (refer to Appendix B). Peaks near 3400 cm^{-1} represent -OH groups of alcohol (Shakya et al., 2022), near 2900 cm^{-1} could be due to stretching vibrations of $-CH_2$ (Chen et al., 2008; Wang et al., 2020). Stretching near 1600 cm^{-1}, 1400 cm^{-1} and 1000 cm^{-1} peaks may correspond to -C=O, -COO and -C-O, respectively (Chen et al., 2008; Shakya et al., 2022).

7.16 Water absorption capacity and mechanical strength of beads

The water absorption capacity and mechanical strength were used to assess the structural stability of the beads. Absorption for both beads, IBK and IBT, were almost similar. There was a negligible increase in weight (<1%) for the first two days before reaching a maximum value after five days. The maximum absorption observed was 5.82% for IBK and 6.48% for IBT beads (refer to Appendix D). A high degree of swelling reduces the mechanical strength and stability of beads.

Mechanical strength test revealed that after 48 h, out of 20, only two beads ruptured in both cases with a ratio of 0.9 [(number of beads ruptured)/(total number of beads)]. It employed that the beads prepared were of higher grade and had good mechanical strength and stability. Good mechanical strength also showed high cross-linking density (Zhang et al., 2022), resulting in better-quality beads.

7.17 Reusability of the beads

The reusability of beads is an important parameter to assess their economic viability, as reusability can significantly reduce the cost of treatment. To check their reusability, the beads were filtered from the solution, immersed in distilled water, kept for 24 h at 100 rpm, and washed thrice before their reuse for the next cycle. IBK and IBT were effectively reusable for up to five cycles, whereas IBK+IBT was effective for up to eight cycles for

As(V) and seven cycles for As(III), before the removal efficiency dropped to below 80%. The efficiency in the case of IBK [for As(V)] decreased from 93.51 ± 0.36% to 85.87 ± 0.66%, whereas for IBT [for As(III)], the decrease was from 91.75 ± 0.89% to 81.24 ± 0.61% after five cycles (Figure 7.8). But in the sixth cycle, the efficiency dropped to 75.94 ± 0.82% and 74.08 ± 0.72% for IBK and IBT, respectively. With IBK+IBT, the decrease was from 94.04 ± 0.05% to 72.04 ± 0.42% for As(V) in the ninth cycle and from 94.08 ± 0.05% to 76.64 ± 0.32% in the eighth cycle for As(III). However, efficiency dropped below 50% for IBK and IBT after 8 cycles and after 12 cycles for IBK+IBT.

Isawi (2020) reported reusability of up to ten cycles for PVA/SA beads used to remove various heavy metal(loid)s. SA offers flexibility in hydrated environments and exceptional mechanical strength when combined with PVA (Mok et al., 2020). This enhanced strength makes it possible for beads to be reused multiple times, which may make the treatment process cost-effective and sustainable. Generally, hydrogels that can be reused multiple times limit the maximum swelling degree (Zhang et al., 2022), which is also substantiated in this case with less swelling of beads. The stand-alone PSB for arsenic removal was only effective for three cycles. The disposal of beads after exhaustion is a challenge and warrants further investigation.

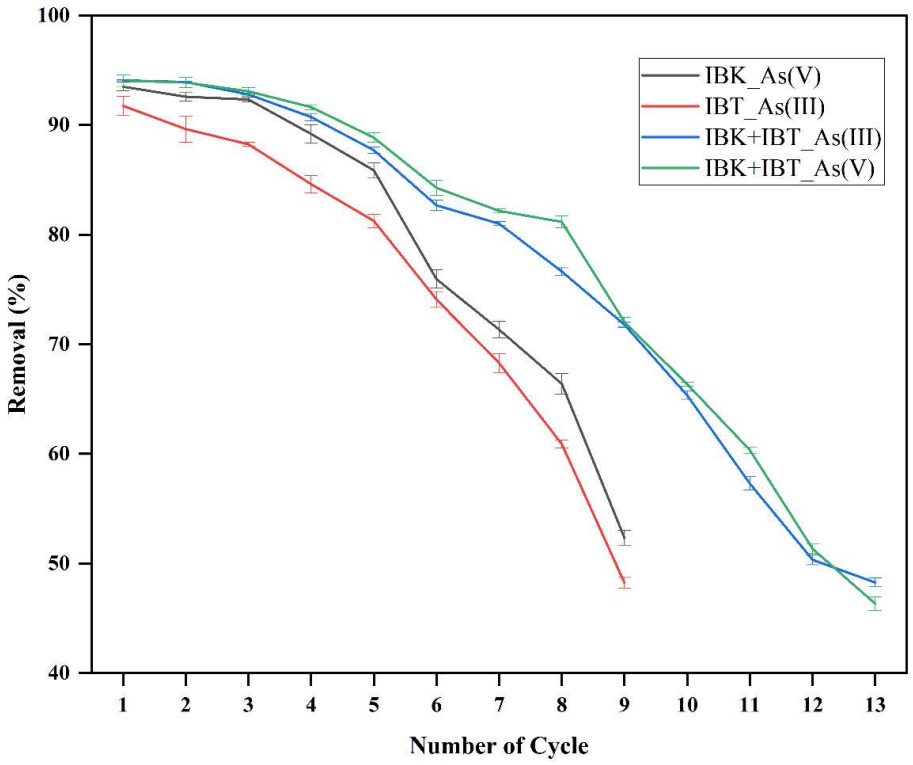

Figure 7.8: Reusability effect on removal efficiency of IBK, IBT and IBK+IBT beads on As(V) and As(III)

7.18 Arsenic removal in packed bed bioreactor using beads

The experiments were performed at different initial concentrations of 1 mg/L, 5 mg/L and 10 mg/L. It was observed that with the increase in initial concentration, removal efficiency and volume of water treated in each cycle reduced. For removal of As(V) using beads of K7Pb, removal efficiency ranged from 94.97 ± 0.02% to 57.86 ± 2.05%, 98.93 ± 0.01% to 63.55 ± 4.96% and 99.43 ± 0.02% to 64.46 ± 4.81% for initial concentrations of 1 mg/L, 5 mg/L and 10 mg/L, respectively (Figure 7.9). The removal efficiencies varied from 95.01 ± 0.01% to 60.44 ± 3.78%, 98.92 ± 0.02% to 63.14 ± 3.68% and 99.37 ± 0.02% to 62.14 ± 3.83% for initial concentrations of 1 mg/L, 5 mg/L and 10 mg/L, respectively for As(III) treated with beads of TY6 (Figure 7.10).

The volume of water treated for the duration of the experiment was 124 L, 110 L and 98 L for TY6 and 132 L, 122 L and 104 L for K7Pb at initial concentrations of 1 mg/L, 5 mg/L and 10 mg/L, respectively. The reduction in efficiency and volume of water treated may be due to the reduced capacity of bacteria and the decrease of adsorption sites of biochar and beads with each cycle. The beads also showed biotransformation ability. TY6 could oxidize As(III) to As(V) and K7Pb could reduce As(V) to As(III). Beads of TY6 showed a maximum oxidation capacity of 51.26 ± 3.28% (with an initial concentration of 10 mg/L) (Figure 7.11), whereas the maximum reduction obtained was 57.45 ± 2.83% (with an initial concentration of 5 mg/L) with beads of K7Pb (Figure 7.12). It was observed that the reduction and oxidation capability decreased significantly with successive cycles. The maximum oxidation and reduction were 10.76 ± 1.34% and 10.40 ± 1.84%, respectively, in the fifth cycle.

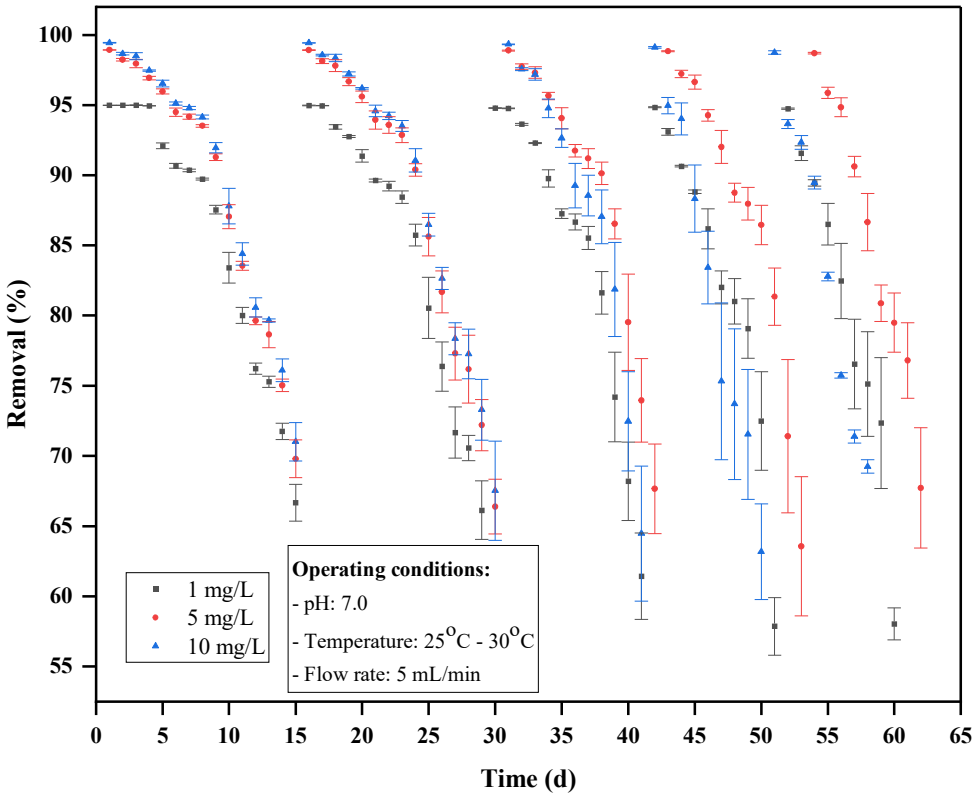

Figure 7.9: Removal of As(V) using beads of K7Pb in RPBBR during different cycles

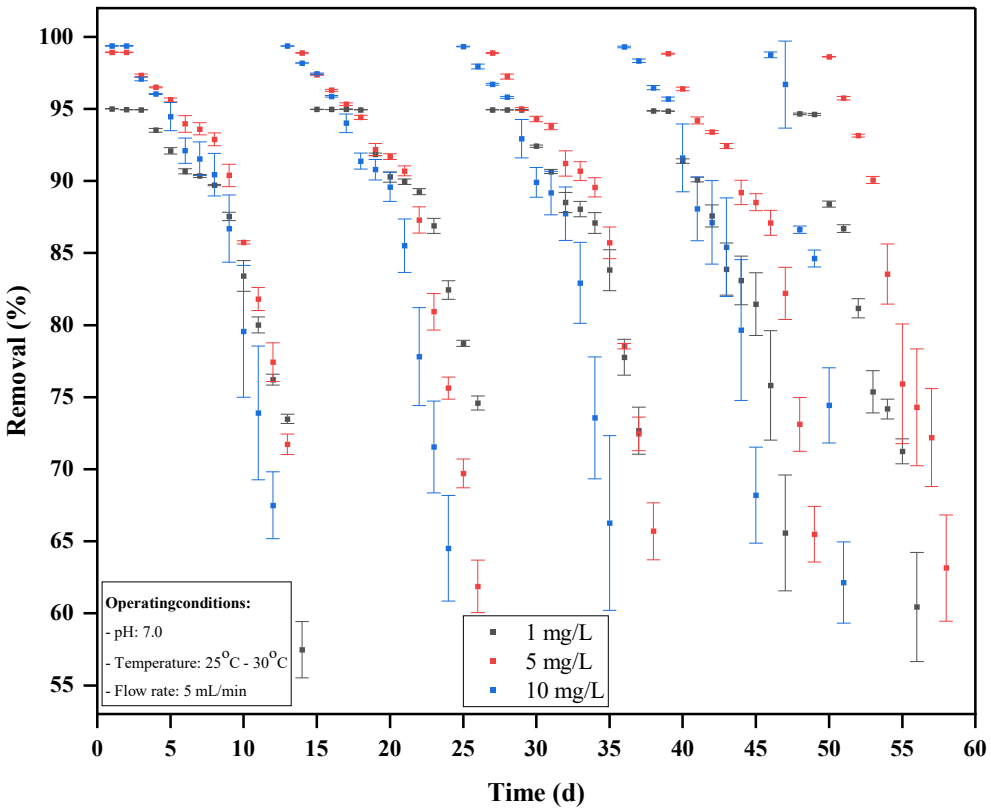

Figure 7.10: Removal of As(III) using beads of TY6 in RPBBR during different cycles

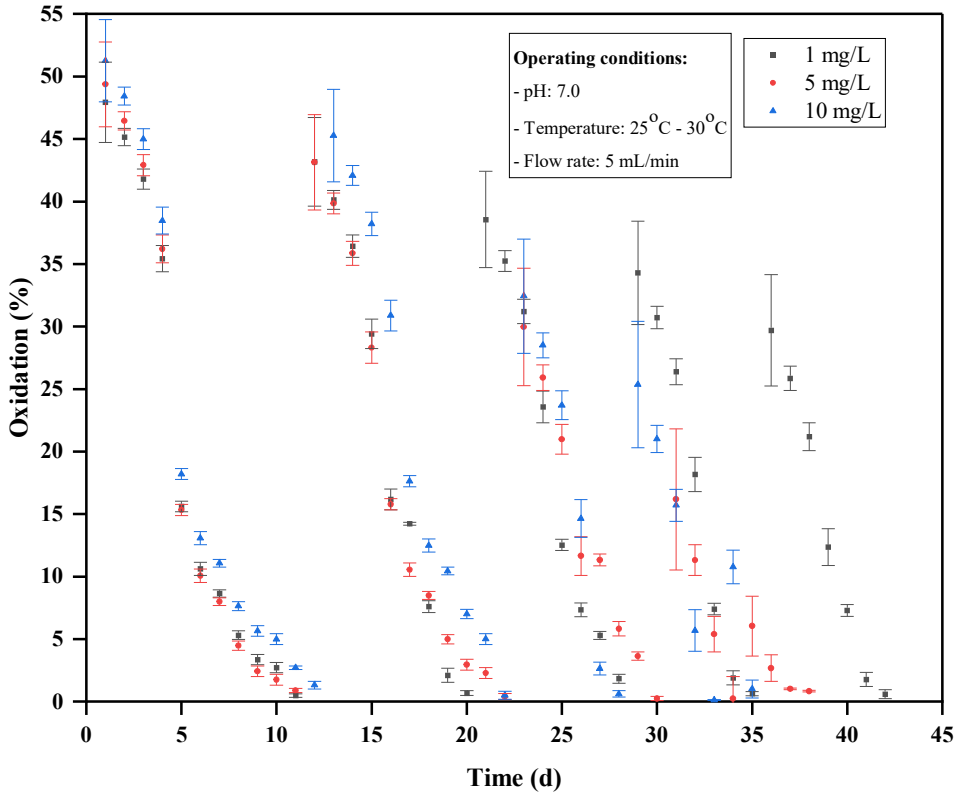

Figure 7.11: Oxidation efficiency of beads of TY6 in RPBBR during different cycles

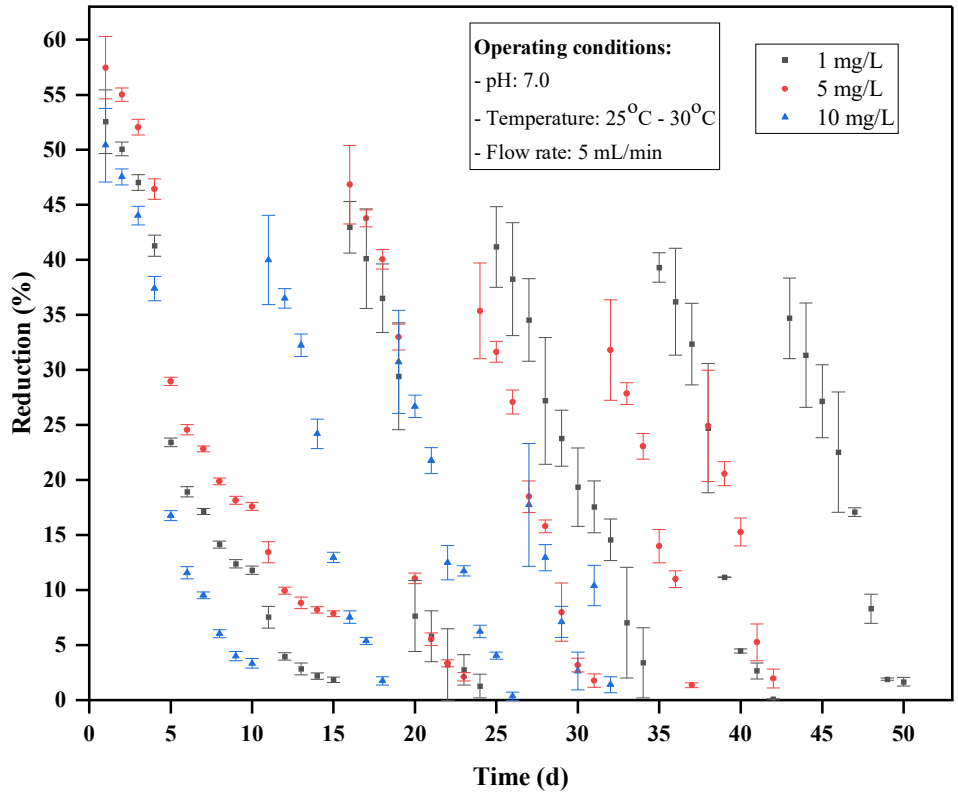

Figure 7.12: Reduction efficiency of beads of K7Pb in RPBBR during different cycles

7.19 Summary

As(III) and As(V) removal efficiency of PSB and MPSB was compared in aqueous solutions. The sorption efficiency of MPSB was relatively higher than that of PSB at pH 6 for As(III) (86%) and for As(V) (91.26%) for an initial concentration of 1 mg/L, adsorbent dose of 0.5 g/L and 240 min equilibrium time at 100 rpm. Freundlich isotherm and pseudo-second order model suggested possible multilayer chemisorption. FTIR spectroscopy showed that –OH, C-C, C=C and C-O-C groups contributed significantly to adsorption for both PSB and MPSB. The thermodynamic study revealed that the adsorption process was spontaneous and endothermic.

PVA-SA beads of bacteria immobilized on PSB were successfully fabricated in the laboratory and were employed for arsenic removal from an aqueous solution. The optimum parameters obtained for the most efficient beads were PVA – 5% (w/v), SA – 2% (w/v) and $CaCl_2$ – 1% (w/v). The arsenic removal efficiency of beads was higher than that of free-cell, biochar, or bacteria immobilized on biochar. As(III) and As(V) removal efficiency varied between 77% - 94% for different combinations of bacteria. Water absorption and mechanical tests revealed that beads had low water absorption capacity (5% - 7%), good stability and mechanical strength. Beads showed good reusability, easy handling and extraction after use. The beads were found to be an environment-friendly approach for treatment of arsenic.